# Road Clutter Spectrum of BSD FMCW Automotive Radar

Yu-Zhen Ma, Chenglin Cui, Byung-Sung Kim,
Information & Communication Engineering
Sungkyunkwan University
Suwon, Republic of Korea
bskimice@skku.edu

Jeong-Min Joo, Seung Hoon Jeon
Research & Development Division
Hyundai Motor Company
Hwaseong, Republic of Korea

Sangwook Nam
Electrical Engineering & INMC
Seoul National University
Seoul, Republic of Korea

***Abstract*—Suppressing road clutter is important for automotive radar signal processing to detect targets, which requires accurate spectral distribution of clutter. This work derives the simple clutter model for FMCW automotive radar and presents experimental results of road clutter spectrum for FMCW blind spot detection (BSD) radar at 24 GHz in various road environments. The measured power spectrum shows the spectrum distribution as the simple theory predicts.**

***Keywords— clutter; spectrum; FMCW; automotive radar; blind spot detection***

## I. INTRODUCTION

Radar detects the target embedded in clutter and noise. Since clutter level is usually higher than thermal noise, accurate clutter modeling is important to improve the detection probability for automotive radars. Since clutter is due to very complex background echoes, clutter modeling is a challenging task for radar system. While numerous modeling and empirical studies of clutter for airborne and static ground radar systems were conducted in the past [1-5], only few studies provide information on FMCW automotive radar clutter. Previous researches of automotive radar clutter paid much more attention to mitigation of clutter [6-8].

In this paper, the road clutter spectrum observed by the FMCW radar equipped in the moving vehicle is computed and the results are compared with experimental results measured by commercial BSD radar systems. This paper is organized as follows. Theoretical derivation of the clutter model is described in Section II. Section III presents the measured results from multiple scenarios collected by stationary and moving vehicle equipped with FMCW radar. Finally, conclusion of the implication of this work is provided in Section IV.

## II. THEORY OF AUTOMOTIVE FMCW RADAR CLUTTER

The coordinate geometry of clutter area and some parameters are depicted in Fig.1. The vehicle is moving toward –y direction and the beam of the radar illuminates +y direction for BSD radar operation. But the theory can be extended to forward looking automotive radars.

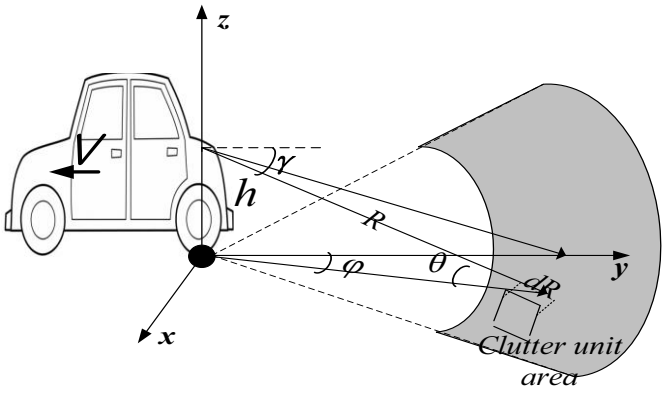


Fig. 1. Geometry of clutter unit among whole clutter area

### A. The static clutter power specturm from range cells

The static clutter power coming from the unit range cell illuminated by the stationary automotive radar is given by [8, 9]

$$dP_{static\_clutter} = K\frac{g(\theta,\varphi)^2}{R^3}\cdot dR\cdot d\varphi \qquad (1)$$

, where $dR$ is the range resolution, $d\varphi$ is azimuth angle resolution, $R$ is the range of the target, $g(\theta,\varphi)$ is the normalized antenna pattern assuming the same antennas for the transmitter and the receiver. $K$ is an amplitude factor defined by

$$K = \frac{P_t G_0^2 \lambda^2 \sigma^0}{(4\pi)^3} \qquad (2)$$

, where $\lambda$ is the wavelength, $\sigma^0$ is the clutter scattering coefficient and $G_0$ is the maximum antenna gain. In the stationary case, the received signals from the same range $R$ have the same amplitude and IF beat frequency. Then, the static power spectral density is obtained by replacing the range $R$ and $dR$ with the corresponding range beat frequency $f_R$ and its differential $df_R$ given by

$$f_R = \frac{2RB}{cT_B} = \alpha_R R,\ \alpha_R = 2B / cT_B \tag{3}$$

$$df_R = \alpha_R dR \tag{4}$$

and integrating over the angle $\varphi$ illuminated by the antenna beam. In (3), $B$ and $T_B$ are the bandwidth and sweep time of the transmitted signal respectively and $c$ is the speed of light. Since the angle $\theta$ is a function of $R$ and therefore the function of $f_R$ , the static clutter spectrum is easily obtained by integrating $\varphi$ for a beamwidth. The static clutter spectrum is centered on DC as found in [8] and given by (6)

$$S(f)_{static} = K\left(\frac{2B}{cT_B}\right)^2 \int \frac{g_1(f_R,\varphi)^2}{f_R^{\,3}} d\varphi \tag{6}$$

, where $g_1$ is the normalized gain function transformed by the coordinate transformation rule.

*B. The Doppler clutter power specturm from isodop contour*

When the vehicle is moving with a speed, the radar receives a large number of echoes with random amplitudes, phases, and angle of arrivals relative to the direction of the vehicle motion. The relative direction between the radar and each clutter cell causes the Doppler shifted frequency. When the transmitted signal is CW without frequency sweep, this spreading phenomenon is similar to that of the deep fading environment encountered in mobile radio channels [10]. Doppler clutter is caused by the relative motion between the vehicle and the ground. Due to the elevation of the radar antenna from the ground, the angle $\gamma$ is continuously changed along the range. Therefore, the Doppler frequency is also changed for the same grazing angle $\theta$. To obtain the Doppler power spectrum, it is necessary to combine the power from the range cells which gives the same Doppler shift frequency.

$$f_d = f_m \cos\gamma = f_m \cos\theta\cos\varphi \tag{7}$$

In (7), $f_m$ is the maximum Doppler frequency given by $2v_{veh} / \lambda$, where $v_{veh}$ the speed of the vehicle. Clutter echoes from all cells with the same $\gamma$ show the same frequency shift. These points form a hyperbolic contour of equal Doppler frequency shift, called an isodop [11].

To obtain the Doppler clutter spectral density, change of integration variable from $\varphi$ to $f_d$ in (1) is essential. Since the angle $\theta$ is a constant for a given range $R$, $d\varphi$ can also be expressed using $f_d$ as follows

$$df_d = -f_m \cos\theta \sin\varphi d\varphi \tag{8}$$

By substituting (8) into (3), the received power from unit cell becomes a function of $R$ and $f_d$ as follows

$$dP_{Doppler\_clutter}(R, f_d) = K\frac{g(\theta,\varphi)^2}{R^3}\frac{1}{\sin\varphi\cos\theta}\cdot\frac{dR}{f_m}df_d \tag{9}$$

The integration (9) along the range for isodop contour results in the Doppler clutter spectral density below.

$$S_{Doppler}(f)df_d = K\int_{R_{\min}}^{R_{\max}} \frac{g_2(R,f_d)^2}{R^3}\sqrt{\frac{R^2}{R^2\left(1-\left(f_d/f_m\right)^2\right)-h^2}}\cdot\frac{dR}{f_m}df_d \tag{10}$$

In (10), $g_2$ is the normalized gain function transformed by the coordinate transformation rule and $R_{\min}$ is the minimum range that yields $f_d$ at $\varphi = 0$ and given by

$$R_{\min} = \sqrt{\frac{h^2}{1-\left(f_d/f_m\right)^2}} \tag{11}$$

The Doppler spectrum is strongly dependent on the antenna beam pattern as demonstrated in [10]. For the narrow beam pattern centered around $\theta = 0°$ , the spectral density monotonically increases and has the peak at $f_d = f_m$

*C. The FMCW radar clutter power specturm*

The FMCW radar in the moving vehicle yields the IF frequency which is the sum of the range beat frequency and the Doppler shifted frequency.

$$f_{IF} = f_R + f_d \tag{12}$$

In (12), without loss of generality, the positive shift is only considered. As shown in Fig. 3, the circular contour gives the constant range beat frequency $f_R$ and the hyperbolic contour yields the constant Doppler echoes with $f_d$ . Therefore, a constant IF frequency $f_{IF}$ is generated by many intersections of range contour and isodop contour. For the contour of large $f_R$, the intersection cell A is made by the small $f_d$ contour as shown in Fig. 2 and vice versa as the point B. In addition, there is a minimum range that can yield $f_{IF}$ because the small $f_R$ needs the large $f_d$, but each contour moves in the opposite direction. Therefore, the point C is the final intersection that gives the same IF frequency. The clutter spectral density can be obtained by changing the integration variable from $R$ to $f_R$ and $f_d$ to $f_{IF}$ and integrating from $f_{R\min}$ corresponding to $R_{\min}$, as seen in (13).

Fig. 3 shows the calculated IF spectral density normalized by $K$ factor assuming Gaussian beam elevation pattern with 3dB beamwidth of 30° and uniform illumination for azimuthal angle. As can be seen in the figure, the spectral density shows monotonic increase and abrupt decrease around the maximum Doppler frequency which is well matched to measurement results as found in Section III.

$$S_{FMCW}(f_{IF})df_{IF} = K\int_{f_{R\min}}^{f_{IF}} \frac{g_3(f_R,f_{IF})^2}{\left(f_R/\alpha_R\right)^2}\sqrt{\frac{1}{\left(f_R/\alpha_R\right)^2\left(1-\left(\left(f_{IF}-f_R\right)/f_m\right)^2\right)-h^2}}\cdot\frac{df_R}{\alpha_R f_m}df_{IF} \tag{13}$$

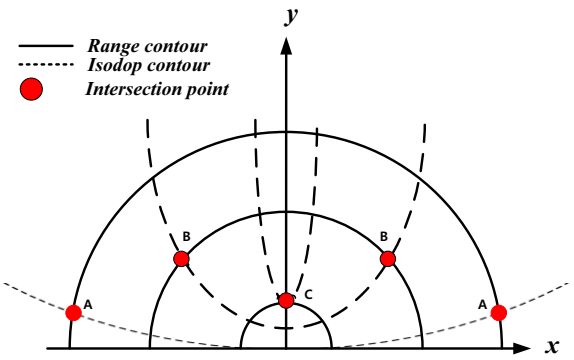


Fig. 2. Intersection points of range and isodop contours yielding equal IF

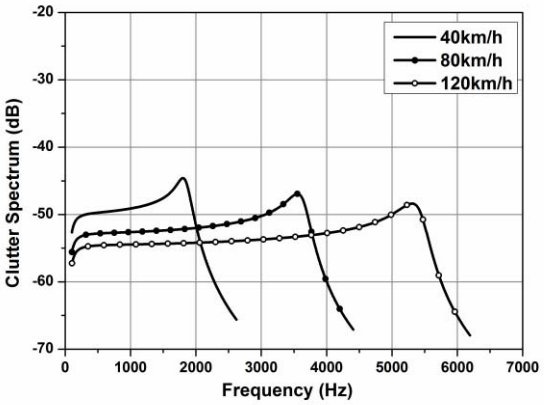


Fig. 3. Ground clutter spectrum for FMCW radar moving with a speed of 40 km/h, 80 km/h and 120 km/h respectively. $T_B$ =40ms, B=100MHz.

## III. MEASUREMENTS

A commercial 24GHz FMCW radar system for blind-spot detection from Hyundai Motor Company is used for clutter measurement. The radar system is equipped in the rear bumper of a sedan. The detection range is up to 70 meters, but unfortunately detailed system characteristics are unavailable. The radar system uses 24.15~24.25GHz frequency range and 40-msec ramp time to form a FMCW chirp signal.

### *A. Experimental results of stationary clutter*

To confirm the validness of the presented Doppler clutter model, both stationary and moving state experiments were carried out. The experiment was accomplished in a park with concrete ground and there are no obstacles near the vehicle. The real-time beat signal is sampled and stored for later processing. The power spectral density (PSD) is obtained using Fourier transform of the IF output. The measurement results under stationary condition are depicted in Fig. 4 (a). The bold line represents the average of the acquired data for several chirping periods while the fine line is plot of the maximum. The maximum range beat frequency of 70-meter range is 1.17 kHz. Therefore frequency components beyond this frequency are ignored. Most of the static clutter is concentrated around DC to 200Hz. Since the spectrum is composed of system noise and clutter echo, it is difficult to exactly determine the static clutter level. The stationary clutter level is regarded as a reference for moving clutter.

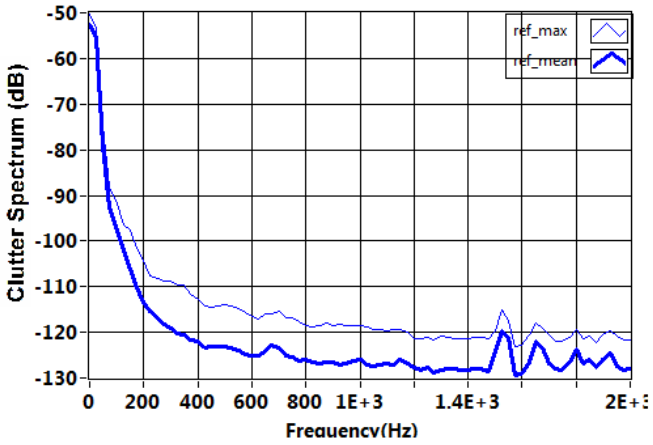


(a)

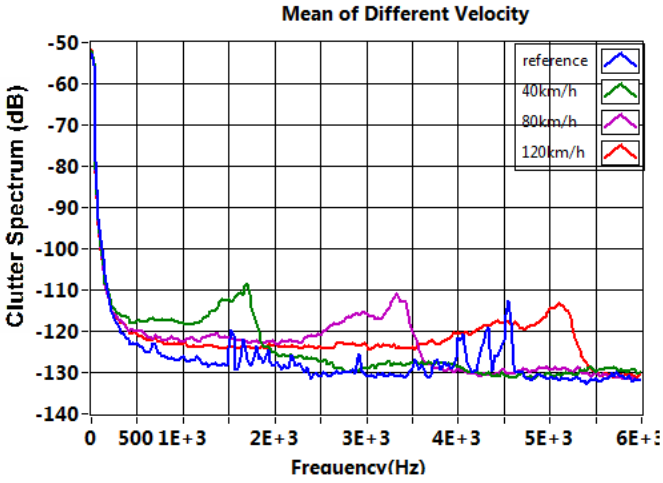


(b)

Fig. 4. Measuremental results of (a) stationary clutter and (b) moving clutter with three kinds of velocities.

### *B. Experimental results of moving clutter*

In order to observe moving clutter, driving experiment is carried out at the same environment with three different speeds around 40Km/h, 80Km/h and 120Km/h. Fig.4 shows clear Doppler frequency shift with different velocities of the vehicle. The spectrum distribution is not symmetric around the Doppler frequency. Instead, the spectrum shows a gradual increase before and sharp decrease after the maximum Doppler frequency. These characteristics are all the same with three different speeds as predicted by the moving clutter model.

Additionally, several experiments under different road conditions are carried out and one of them is shown in Fig. 5. The measurement results are shown in Fig.6. Clutter shows similar characteristics with previous measurement results but the Doppler clutter level is much higher than former ones. Though the different ground condition and the roadside environment may result in the increase of clutter level, the spectrum distribution looks similar to that of the flat ground condition.

Fig. 5. One of the road conditions for BSD radar experiments.

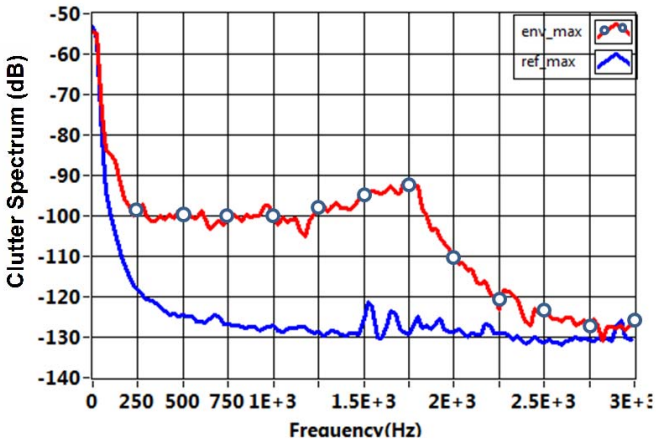


Fig. 6. Experimental results of moving clutter using BSD radar for the environment seen in Fig. 5 when the speed is around 40Km/h. The level of clutter is much higher than the flat ground condition.

## IV. CONCLUSION

The analysis and experiment results of clutter spectral density for FMCW automotive radar is illustrated in this work. The model and measurement results show the gradual increase and rapid decrease of the spectrum distribution around the maximum Doppler frequency for flat ground condition. Similar spectrum distribution was observed for complex road environments but with higher clutter level.


## ACKNOWLEDGMENT

This work is supported by Hyundai Motor Company for providing funding and facilities to carry out this research and the National Research Foundation of Korea (NRF) grant funded by the MSIP and the MEST (No. 2009-0083495, 2013-056424).


## REFERENCES


[1] A. L. Friendlander, and L. J. Greenstein, “A Generalized Clutter Computation Procedure for Airborn Pulse Doppler Radars,” in IEEE Transactions on Aerospace and Electronic Systems, vol. AES-6, no. 1, pp. 55-61, 1970.

[2] Al-Ashwal, W. A., Baker, C. J., Balleri, A., Griffiths, H. D., Harmanny, R., Inggs, M., Miceli, W. J, et al, “Statistical analysis of simultaneous monostatic and bistatic sea clutter at low grazing angles,” Electronics Letters, vol. 47, no. 10, pp. 621-622, May 2011.

[3] E.G. Hoare, L.Y. Daniel, M. Gashinova, K. Kabakchiev, V. Sizov, M. Cherniakov, V.B.Razskazovsky, G.I.Khlopov, S.I.Khomenko and V.E.Morozov, “Near Zero Grazing Angle Forward-Scatter Sea Clutter Measurement Spectrum Analysis” in IET Radar 2012 Conference, Glasgow, October 2012.

[4] J. B. Billingsley, A. Farina, F. Gini, M. V. Greco, and Verrazzani, L. “Statistical analyses of measured radar ground clutter data,” IEEE Transactions on Aerospace and electronic Systems, vol. 35, no. 2, pp. 579-593, Apr 1999.

[5] X. Liu, Y. Li and Y. Cheng, “The analysis of the side-lobe clutter in the pulse,” Journal of Computational Information Systems, vol. 8, no. 4, pp. 1671-1677, 2012.

[6] J. Yu and J. Krolik, “MIMO multipath clutter mitigation for GMTI automotive radar in urban environments,” in IET Int. Conf. Radar Systems, pp. 1–5, 2012.

[7] H. Rohling, “Radar CFAR Thresholding in Clutter and Multiple Target Situations,” IEEE Transactions on Aerospace and Electronic Systems, AES-19, pp. 608-621, July 1983.

[8] S. Halai, P.V. Brennan, D. Patrick and I. Weller, "Frequency shifted active target for use in FMCW radar systems," in IEEE Radar Conference, pp. 0819-0823, 2014.

[9] G. P. Kulemin and D. K. Barton, Millimeter-wave radar targets and clutter. Artech House, 2003.

[10] M. J. Gans, “A Power-Spectral Theory of Propagation in the Mobile-Radio Environment,” in IEEE Transactions on Vehicular Technology, vol. VT-21, no. 1, pp. 27–38, Feb 1972.

[11] A. L. Friendlander, and L. J. Greenstein, “A Generalized Clutter Computation Procedure for Airborn Pulse Doppler Radars,” in IEEE Transactions on Aerospace and Electronic Systems, vol. AES-6, no. 1, pp. 55-61, 1970.